Journal of Engineering Mechanics and Machinery (2025)
Clausius Scientific Press, Canada

DOI: 10.23977/jemm.2025.100114
ISSN 2371-9133 Vol. 10 Num. 1

Sound Transmission Performance of a Ventilated Acoustic Metastructure Composed of Helmholtz Resonator and Thin Membrane

Qi Liu, Rurui Huang, Lei Shi, Ni Zhen*

School of Mechanical Engineering, Tianjin University of Science and Technology, Tianjin, 300222, China
**Corresponding author: zhenni@tust.edu.cn*

Keywords: Sound Insulation; Ventilation; Helmholtz Resonance; Thin Membrane Resonance; Sound Transmission Loss

Abstract: Traditional soundproofing materials face limitations in meeting modern noise reduction demands, particularly in balancing acoustic performance with ventilation requirements. To address this challenge, we propose a novel acoustic metamaterial composed of a Helmholtz resonance cavity coupled with a thin-membrane structure. This hybrid design achieves simultaneous sound insulation, noise reduction, and effective airflow circulation. Numerical results demonstrate that the composite structure exhibits significant low-frequency sound attenuation, with over 10dB of sound transmission loss in low-frequency range of 70~230Hz. Remarkably, the system maintains a peak sound transmission loss of up to 65dB while preserving ventilation functionality. This work also investigates the influence of key geometrical parameters on sound transmission performance of the metastructure. This work provides a promising solution for applications requiring both acoustic control and air circulation in low-frequency range.

1. Introduction

Noise pollution has emerged as a critical environmental challenge, significantly impacting both daily life and occupational environments[1][2]. Chronic exposure to noise pollution has been clinically associated with various adverse health effects, including nausea, tinnitus, and neurasthenia[3][4]. In conventional noise control approaches, materials such as soundproof glass and acoustic panels demonstrate effective noise attenuation[5][6]. However, these traditional materials present a few main limitations, such as excessive weight and bulkiness, poor low-frequency sound insulation performance[7][8], and an inherent trade-off between ventilation and acoustic insulation properties[9]. Therefore, it is crucial to conduct more research on new sound insulation materials.

Recent advances in acoustic metamaterials and metasurfaces have provided innovative solutions to circumvent the inherent limitations of conventional sound-absorbing materials[10][11][12], leading to the development of diverse acoustic units[13][14][15]. Several resonance mechanisms have been applied in the designs, including Helmholtz resonance, Fabry-Pérot resonance, Fano

resonance, and Membrane resonance, etc. Resonators based on each mechanism exhibit unique frequency-dependent characteristics, making them particularly suitable for different acoustic control scenarios. Helmholtz resonators[16][17][18] attenuate acoustic energy through cavity resonance, with primary dissipation occurring via thermoviscosity friction at the neck region. In contrast, membrane-based acoustic absorbers[19][20][21], employ elastic membranes coupled with mass-loaded elements, where resonant frequency tuning is achieved through membrane tension adjustment, enabling effective low-frequency sound absorption. Spatially coiled metamaterials, usually based on Fabry-Pérot resonance or Fano resonance[22][23][24], facilitate low-frequency sound insulation by extending the acoustic propagation path, thereby promoting enhanced acoustic energy dissipation.

Building upon the comparative analysis of existing ventilated acoustic metastructures[25], we propose a novel composite metastructure that synergistically integrates a Helmholtz resonator with a thin membrane to simultaneously achieve sound insulation and ventilation in this paper. The hybrid-resonance based design combines compact dimensions and lightweight characteristics with exceptional acoustic performance, demonstrating over 10 dB of sound transmission loss in the 70-230 Hz low-frequency range while maintaining effective air permeability. The successful implementation of this ventilated acoustic metastructure presents significant potential for industrial applications where both noise control and airflow circulation are critical requirements.

2. Metastructural design and theoretical study of acoustic ventilation

2.1. Metastructural design

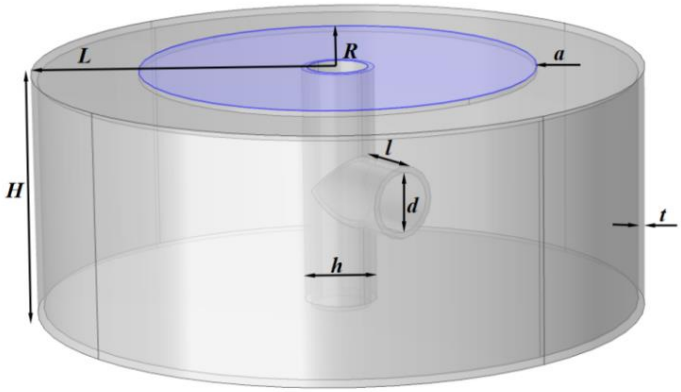

Figure 1 3D view of the metastructure

The three-dimensional diagram of the proposed Helmholtz resonator-thin membrane composite metastructure is shown in Figure 1. The overall radius L of the metastructure is 50mm, the overall thickness H is 40mm, the diameter h of the central cylindrical vent is 10mm, and the wall thickness t of the metastructure is 1mm. The metastructure as a whole can be divided into two regions, the first region is the grey region in the figure for the Helmholtz cavity structure, the material is epoxy resin and the length l of the protruding neck is 10 mm, and similarly the diameter of the neck d is 10mm. The second region is the blue region for the membrane structure, the membrane has a central opening of the same size as the vent, the membrane radius size R is 32.5 mm, and the membrane thickness a is 0.1 mm. The membrane material is made of polyetherimide(PEI) and its material parameters are given in Table 1.

Table 1 Structural Material Parameters

Material	PEI membrane	Epoxy resin
Young modulus(MPa)	4	2.6
Density(kg/m^3)	1380	1130
Poisson ratio	0.3	0.4

2.2. Sound insulation theory and finite element modeling

The propagation control equation of the sound in the air domain is[26]:

$$\nabla \cdot \left(-\frac{1}{\rho_0} \nabla p - \frac{\omega^2 p}{\rho_0 c_0^{\ 2}} \right) = 0 \tag{1}$$

Among them,
p-----the sound pressure;
ρ_0------the air density;
c_0------the speed of sound in the air;
The equation of control for the acoustic wave propagation in the structure can be expressed as:

$$(\lambda + \mu)\nabla(\nabla \cdot \mathbf{u}) + \mu \nabla^2 \mathbf{u} + \rho \omega^2 \mathbf{u} = 0 \tag{2}$$

Where, $\mathbf{u}$ is the displacement vector, λ and μ are the first and second Lame constants of the structural material, respectively. The Lame constants can be associated to the Young's modulus and Poisson's ratio, as shown in the following equation:

$$\lambda = \frac{E\nu}{(1+\nu)(1-2\nu)}, \mu = \frac{E}{2(1+\nu)} \tag{3}$$

At the air/structure interface, the boundary conditions are:

$$\frac{1}{\rho_0} \frac{\partial p}{\partial n} = \omega^2 u_n, \quad T_{ij} n_j = p\mathbf{n} \tag{4}$$

Among them,
u_n ------ the normal displacement of the solid boundary;
$\mathbf{n}$ ------ the normal unit vector oriented in the air domain;
T_{ij}------the Cauchy stress tensor.
The boundary condition make sure the coupling of elastic waves in the metastructure and acoustic waves pressure in the air. Then the discrete form of the acoustic elastic equation can be shown as[27]:

$$\begin{pmatrix} \mathbf{K}_s & \mathbf{S}_{fs}^T \\ \mathbf{0} & \mathbf{K}_f \end{pmatrix} \begin{pmatrix} \bar{\mathbf{u}} \\ \mathbf{p} \end{pmatrix} - \omega^2 \begin{pmatrix} \mathbf{M}_S & \mathbf{0} \\ -\mathbf{S}_{fs} & \mathbf{M}_f \end{pmatrix} \begin{pmatrix} \bar{\mathbf{u}} \\ \mathbf{p} \end{pmatrix} = \begin{pmatrix} \mathbf{F} \\ \mathbf{0} \end{pmatrix} \tag{5}$$

$\bar{\mathbf{u}}$ and $\mathbf{p}$ represent the displacement and the pressure at the grid nodes, respectively. $\mathbf{F}$ is the node force. $\mathbf{K}_s$ and $\mathbf{K}_f$ are the stiffness matrix of the structure and the air. $\mathbf{M}_S$ and $\mathbf{M}_f$ are the

quality matrix of the structure and the air. $\mathbf{S}_{fs}$ represents the fluid-solid coupling matrix, and $\mathbf{S}_{fs}^{T}$ is the transpose matrix of $\mathbf{S}_{fs}$.

In this paper, the material parameters of the air are the density $\rho_0 = 1.21\mathrm{kg}/m^3$ and air velocity $c_0 = 343m/s$, specific heat ratio $\upsilon_0 = 1.4$, air viscosity $\eta_0 = 1.813\times10^{-5}\mathrm{Pa}\cdot s$, thermal conductivity $\kappa_0 = 0.025W/(m\cdot k)$, specific volume heat $C_\Gamma = 0.712kJ/(kg\cdot k)$, At each end of the air domain structure use plane wave radiation boundary condition with incident amplitudes on the left. Sound transmission loss (STL) can be written as:

$$STL = 10\lg\left|P_i/P_t\right|^2 \tag{6}$$

P_i------the amplitude of the incident acoustic pressure;

P_t------the amplitude of the transmitted acoustic pressure.

The finite element analysis software COMSOL Multiphysics is used to simulate the sound transmission loss (STL) of the acoustic ventilation metastructure. Considering the characteristics of the structure design, the thermal viscosity of the air and the deformation of the membrane structure have a large influence on the transmission loss, so the pressure acoustics module, the solid mechanics module and the thermal viscosity module of COMSOL Multiphysics are used simultaneously to perform the simulation calculation of the transmission loss of the acoustic ventilation metastructure. As shown in Figure 2, two air domains are added at each end of the structure to simulate the incoming and outgoing acoustic fields. The plane wave radiation boundary condition is then used to simulate the incident sound wave. In solid mechanics, fixed constraints are imposed around the membrane and a prestress is applied to the domain. Finally, the computational domain is meshed and calculated numerically.

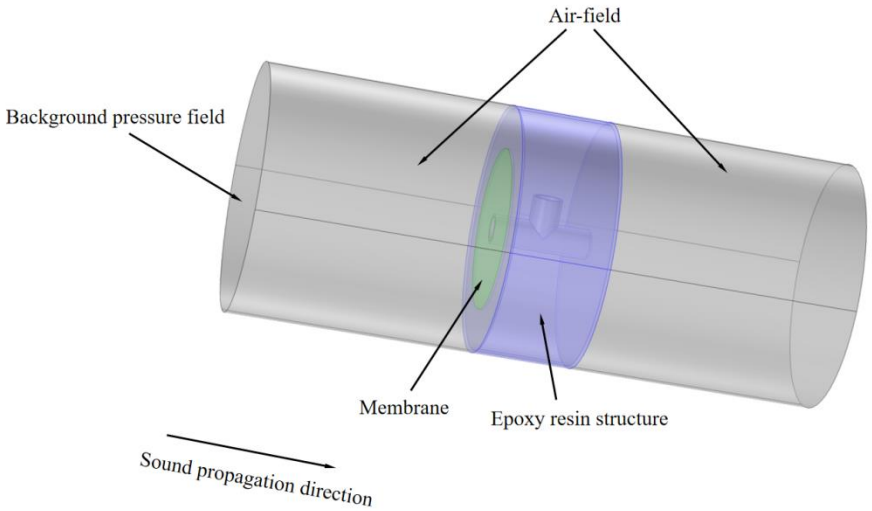

Figure 2 Schematic diagram of the simulation model

By simulating the Helmholtz cavity structure, the thin membrane-cavity structure, and the composite Helmholtz cavity - thin membrane metastructure, as well as the mass law, respectively,

the sound transmission loss-frequency results are plotted in Figure 3. From the figure, it can be seen that the blue curve**,** representing the composite metastructure exhibits better sound insulation performance at lower frequencies than the two non-composite structures, and it achieves a sound transmission loss exceeding 10 dB in the frequency range of 70–230 Hz, and at the same time, and exhibits a broad sound insulation plateau in the range of 400–1000 Hz. Although the peak sound transmission loss of the two non-composite structures is slightly higher than that of the composite metastructure, the overall sound insulation performance of the composite metastructure remains superior and more effective. The sound pressure transmission loss at 200 Hz for this construction is shown in Figure 4. The red region on the left represents the incident sound field. After the sound wave passes through the metastructure model in this paper, part of the sound wave is reflected back, part of the energy of the sound wave is consumed, and part of the sound wave is transmitted directly through the vents. As a result, the outgoing sound field sound pressure is almost zero.

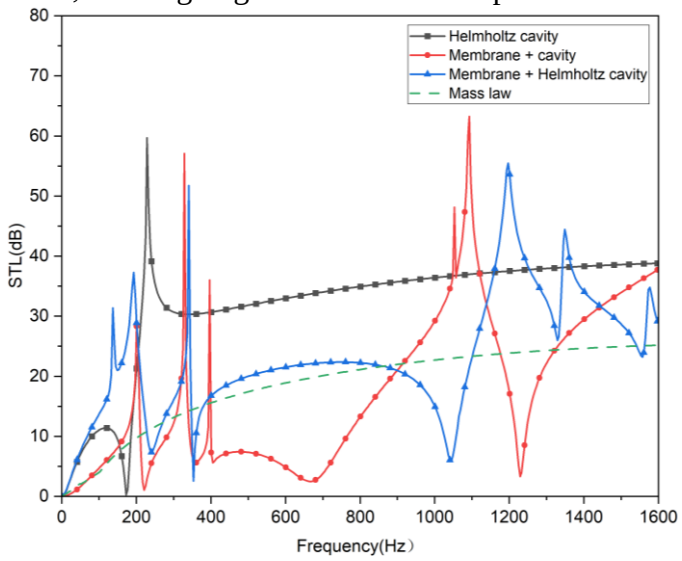

Figure 3 Basic comparison diagram

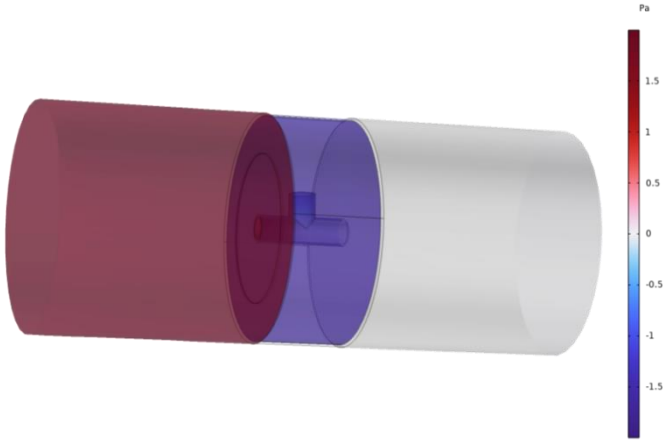

Figure 4 Sound pressure of the model at 200Hz

3. Geometric parameters of composite metastructures

The resonant frequency of the Helmholtz resonant cavity as a function of each geometrical parameter[28] is shown in Equation (7).

$$f_{\text{Helmholtz}} = \frac{c}{2\pi}\sqrt{\frac{S}{lV}} \tag{7}$$

Where,

c------the speed of sound;

S------the neck area $\pi(d/2)^2$;

l------the neck length;

V------the Helmholtz resonant cavity volume.

In general, we only change the neck area and neck length for parametric studies, and we usually do not change the resonant cavity volume as a study, because changing the structure volume is more complicated in practical applications.

The relationship between the resonance frequency of the circular membrane and each geometric parameter is shown in Equation (8)[29].

$$f_{\text{membrane}} = \frac{\mu_n}{2\pi R}\sqrt{\frac{T_0}{\sigma}} = \frac{\mu_n}{2\pi R}\sqrt{\frac{T_0}{a\cdot\rho_{membrane}}} \tag{8}$$

Where μ_n is the root of the zero order Bessel function, R is the radius of the circular membrane, T_0 is the membrane tension (N/m), σ is the membrane surface density, a is the thickness of membrane and $\rho_{membrane}$ is the density of membrane(kg/m^3).

According to Equation (7) and Equation (8), the effects of the following variations of structural geometric parameters on sound transmission loss as well as frequency are investigated.

3.1. Effect of the neck length l of the Helmholtz resonance cavity

With the other geometric parameters kept constant and the neck length *l* is set to 30 mm, 15mm, 10mm and 5mm respectively, the sound transmission loss is simulated and the results are shown in Figure 5.

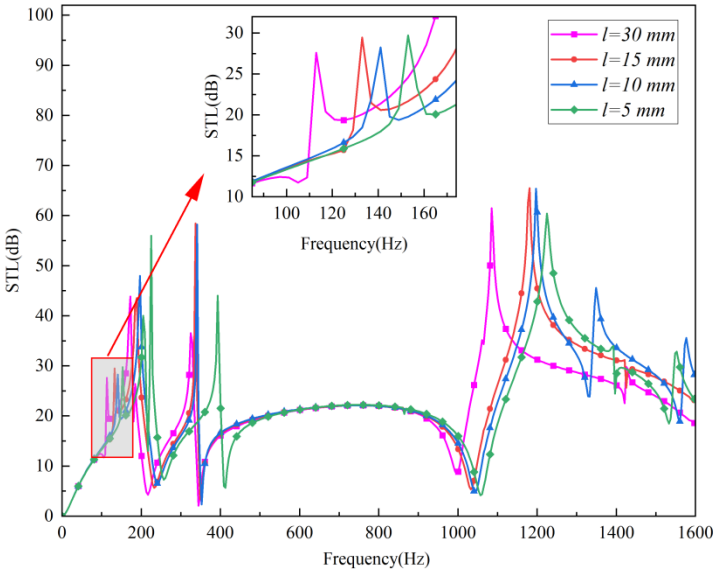

Figure 5 Effect of neck length l on frequency-sound transmission loss

It can be observed that the first peak frequency of the sound transmission loss shifts further toward lower frequencies as the neck of the Helmholtz resonator becomes longer, which also

corresponds to the linear relationship between l and F in Equation (7). Therefore, to achieve sound insulation and noise reduction at low frequencies, the neck length can be increased.

3.2. Effect of the neck area of the Helmholtz resonance cavity

When the diameter d of the circular neck of the Helmholtz cavity is set to 10 mm, 6 mm and 3 mm, respectively, and the other structural parameters remain unchanged, it is found that when the neck area is smaller, the first peak frequency will be at a lower frequency to achieve acoustic noise reduction, but at the same time the peak of the sound transmission loss will also be reduced, making it necessary to select an appropriate size based on different operational requirements. The simulation results are shown in Figure 6.

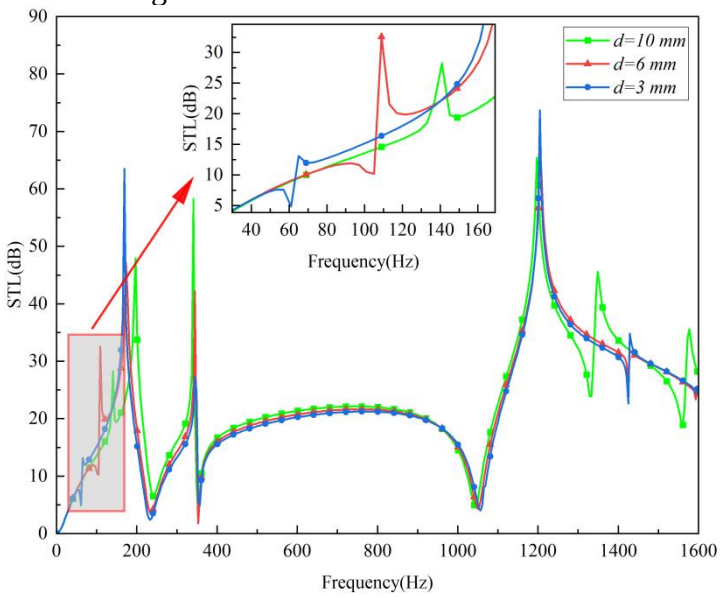

Figure 6 Effect of neck area on frequency-sound transmission loss

3.3. Effect of the neck shape of the Helmholtz resonance cavity

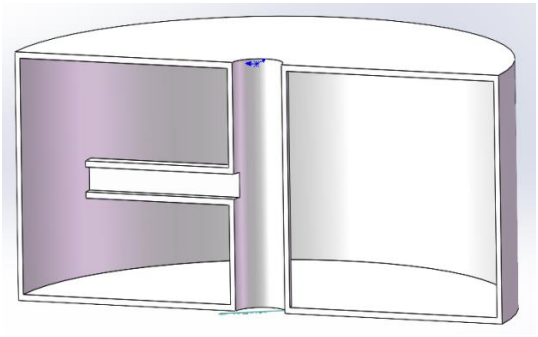

Figure 7 Rectangle neck half-section diagram

When the shape of the neck is changed from a circular to a rectangular cross-section while maintaining the same area, the three-dimensional half-section is shown in Figure 7, and the corresponding simulation results are presented in Figure 8, and it can be seen that the curve diagrams are almost overlapped, and according to Equation (7), if the neck area remains unchanged, its frequency will not be affected. Therefore, under the condition of the same cross-sectional area, the change of the shape of the neck is not significant in the relationship of the effect of acoustic

transmission loss.

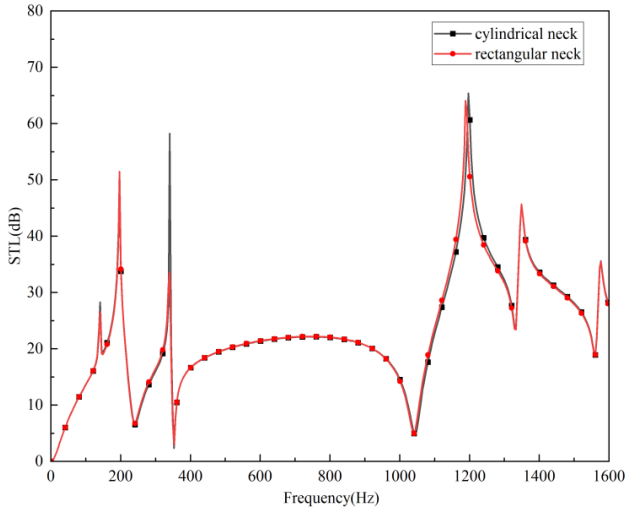

Figure 8 Influence of neck shape on frequency-sound transmission loss

3.4. The effect of the thin membrane thickness a

Changing the membrane thickness *a* also affects the sound insulation, and the corresponding sound transmission loss as a function of frequency is shown in Figure 9.

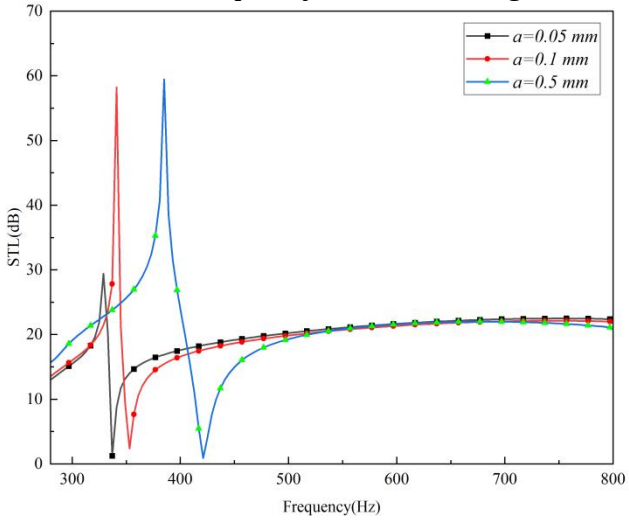

Figure 9 Effect of membrane thickness on the frequency-sound transmission loss

From the figure, it can be seen that as the thickness of the membrane gets thicker, the peak frequency shifts to a higher value, which is in accordance with Equation (8) for the correspondence between the change in membrane thickness and the change in frequency. At the same time, the peak value also increases, this is because the thicker the thickness of the membrane, resulting in the membrane stiffness will be greater, leading to the more sound waves will be reflected. Therefore, when achieving low-frequency sound insulation, thin-membrane thickness can be reduced accordingly.

3.5. Effect of the membrane area

As shown in Figure 10, which illustrates the effect of membrane area variation on sound transmission loss, it can be seen that, while keeping other geometric parameters unchanged, the

larger the membrane diameter *2R* the better sound insulation can be achieved at low frequencies, which is also well in line with the relationship between the variation of the membrane radius and the frequency in Equation (8).

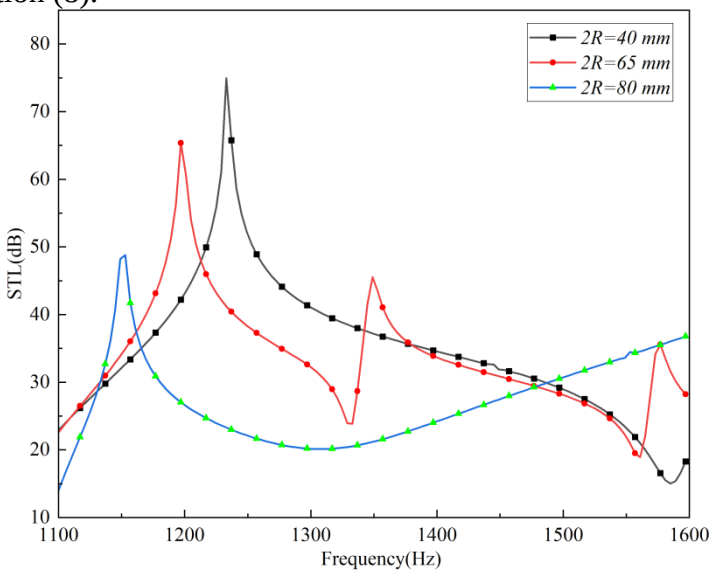

Figure 10 Effect of membrane area on frequency-sound transmission loss

3.6. Effect of the pretensioning T on the frequency-sound transmission loss

Since the membrane needs to be tensioned to exhibit local resonance properties properties and enhance the sound insulation performance of acoustic metamaterials[30], it is necessary to apply pre-stress in the membrane domain. The variation in membrane pre-stress also affects the frequency of sound transmission loss, as shown in Figure 11.

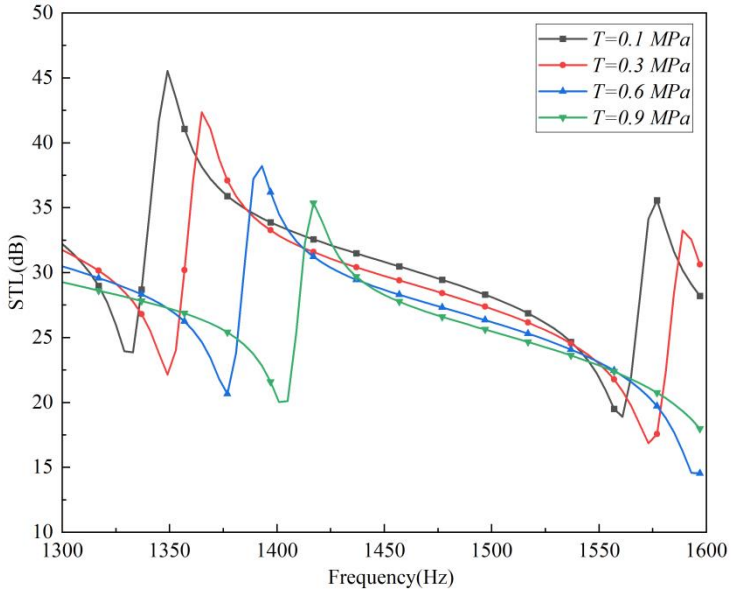

Figure 11 Influence of thin membrane prestress on frequency-sound transmission loss

From Equation (8) and as shown in the figure, it can be observed if other geometric parameters are kept unchanged, the prestressing force *T* become larger and larger, and leading to a corresponding increase in the eigenfrequency of sound transmission loss. The reason why the peak value of the sound transmission loss in Figure 11 decreases with increasing prestressing force is that

there is an opening in the center of the membrane, and as the pre-stress increases, the deformation of the membrane opening becomes more pronounced, allowing more sound waves to be transmitted through the metastructure. As a result, the peak value of the sound transmission loss decreases.

3.7. Effect of the vent size

As shown in Figure 12, increasing the vent diameter *h* to enhance the ventilation rate has a significant effect on the peak sound transmission loss. This is because larger vents allow more sound waves to pass through, thereby reducing the amount of sound insulation. Therefore, the size of the vent should be determined according to the practical requirements to achieve optimal results.

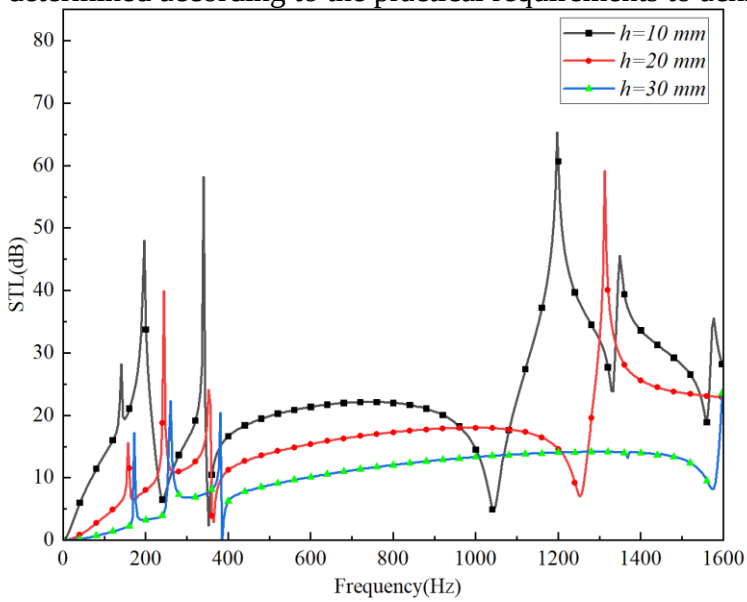

Figure 12 Influence of different vent sizes on frequency-sound transmission loss

4. Conclusion

In summary, this paper proposes a Helmholtz resonant cavity and thin-membrane composite metastructure, which achieves a sound transmission loss of more than 10 dB in the low-frequency range from 70 Hz to 230 Hz, an ultra-wideband platform with a sound transmission loss of 20 dB from 400 Hz to 1000 Hz, and a high transmission loss of more than 20 dB in the mid-to-high frequency range from 1200 Hz to 1600 Hz, with a maximum peak sound transmission loss of 65 dB. By analyzing the effects of different structural geometries on the sound transmission loss across frequencies, the geometrical parameters of the metastructure can be optimized according to the actual needs to achieve the best sound insulation and ventilation results. The metastructure's excellent performance shows great promise in industrial production, aerospace and other fields.

References

[1] Morillas, J. M. B., Gozalo, G. R., González, D. M., Moraga, P. A., & Vílchez-Gómez, R. (2018). Noise pollution and urban planning. Current Pollution Reports, 4(3), 208-219.
[2] Kumar, S., & Lee, H. P. (2019). The present and future role of acoustic metamaterials for architectural and urban noise mitigations. In Acoustics,1 (3),590-607.
[3] Na Ji. (2008). Noise hazards to human body and protection control technology. China Health Engineering, 7(3): 182-183.
[4] Guimei Guo, Huanzhong Deng , Wei Xiange, et al. (2016). Progress on the effects of noise on human health. Occupational and Health, (5): 713-716.

[5] Assouar, B., Liang, B., Wu, Y., Li, Y., Cheng, J. C. (2018). Acoustic metasurfaces. Nature Reviews Materials, 3(12), 460-472.
[6] Shi, J., Liu, C., & Lai, Y. (2018). Controlling the effective bending stiffness via out-of-plane rotational resonances in elastic metamaterial thin plates. New Journal of Physics, 20(10), 103043.
[7] Xu, C., Ma, G., Chen, Z. G., Luo, J., Shi, J., Lai, Y., & Wu, Y. (2020). Three-dimensional acoustic double-zero-index medium with a fourfold degenerate Dirac-like point. Physical Review Letters, 124(7), 074501.
[8] Yang, Z., Dai, H. M., Chan, N. H., Ma, G. C., & Sheng, P. (2010). Acoustic metamaterial panels for sound attenuation in the 50–1000 Hz regime. Applied Physics Letters, 96(4).
[9] De Salis, M. F., Oldham, D. J., & Sharples, S. (2002). Noise control strategies for naturally ventilated buildings. Building and Environment, 37(5), 471-484.
[10] Yu, X. (2019). Design and in-situ measurement of the acoustic performance of a metasurface ventilation window. Applied Acoustics, 152, 127-132.
[11] Kumar, S., & Lee, H. P. (2020). Labyrinthine acoustic metastructures enabling broadband sound absorption and ventilation. Applied Physics Letters, 116(13).
[12] Iannace, G., Ciaburro, G., & Trematerra, A. (2021). Metamaterials acoustic barrier. Applied Acoustics, 181, 108172.
[13] Gritsenko, D., & Paoli, R. (2020). Theoretical optimization of trapped-bubble-based acoustic metamaterial performance. Applied Sciences, 10(16), 5720.
[14] Park, J., Lee, D., & Rho, J. (2020). Recent advances in non-traditional elastic wave manipulation by macroscopic artificial structures. Applied Sciences, 10(2), 547.
[15] Gao, P., Climente, A., Sánchez-Dehesa, J., & Wu, L. (2019). Single-phase metamaterial plates for broadband vibration suppression at low frequencies. Journal of sound and vibration, 444, 108-126.
[16] Hedayati, R., & Lakshmanan, S. P. (2024). Active Acoustic Metamaterial Based on Helmholtz Resonators to Absorb Broadband Low-Frequency Noise. Materials, 17(4), 962.
[17] Gao, Y. X., Li, Z. W., Liang, B., Yang, J., & Cheng, J. C. (2022). Improving sound absorption via coupling modulation of resonance energy leakage and loss in ventilated metamaterials. Applied Physics Letters, 120(26).
[18] Su, Z., Zhu, Y., Gao, S., Luo, H., & Zhang, H. (2022). High-efficient and broadband acoustic insulation in a ventilated channel with acoustic metamaterials. Frontiers in Mechanical Engineering, 8, 857788.
[19] Du, C., Song, S., Bai, H., Wu, J., Liu, K., & Lu, Z. (2024). An investigation on synergistic resonances of membrane-type acoustic metamaterial with multiple masses. Applied Acoustics, 220, 109988.
[20] Jang, J. Y., Park, C. S., & Song, K. (2022). Lightweight soundproofing membrane acoustic metamaterial for broadband sound insulation. Mechanical Systems and Signal Processing, 178, 109270.
[21] Li, X., Zhao, J., Wang, W., Zhu, L., Liu, Y., & Li, X. (2022). Tunable acoustic insulation characteristics of membrane-type acoustic metamaterials array with compact magnets. Applied Acoustics, 187, 108514.
[22] Chang, L., Jiang, A., Rao, M., Ma, F., Huang, H., Zhu, Z., ... & Hu, Y. (2021). Progress of low-frequency sound absorption research utilizing intelligent materials and acoustic metamaterials. RSC advances, 11(60), 37784-37800.
[23] Liu, C., Wang, H., Liang, B., Cheng, J. C., & Lai, Y. (2022). Low-frequency and broadband muffler via cascaded labyrinthine metasurfaces. Applied Physics Letters, 120(23).
[24] Sun, M., Fang, X., Mao, D., Wang, X., & Li, Y. (2020). Broadband acoustic ventilation barriers. Physical Review Applied, 13(4), 044028.
[25] Ang, L. Y. L., Cui, F., Lim, K. M., & Lee, H. P. (2023). A systematic review of emerging ventilated acoustic metamaterials for noise control. Sustainability, 15(5), 4113.
[26] Gonghuan Du, et al. (2001). Acoustic basis [M]. Nanjing: Nanjing University Press.
[27] Wang, T. T., Wang, Y. F., Deng, Z. C., Laude, V., & Wang, Y. S. (2022). Reconfigurable waveguides defined by selective fluid filling in two-dimensional phononic metaplates. Mechanical Systems and Signal Processing, 165, 108392.
[28] Kumar, S., Xiang, T. B., & Lee, H. P. (2020). Ventilated acoustic metamaterial window panels for simultaneous noise shielding and air circulation. Applied Acoustics, 159, 107088.
[29] Ruan, W. Hu, C. N. (2021). Research on the low-frequency sound insulation of thin-membrane acoustic metamaterials. Machine Design and Manufacturing Engineering, 50(3).
[30] Li, J., Zhou, X., Huang, G., & Hu, G. (2016). Acoustic metamaterials capable of both sound insulation and energy harvesting. Smart Materials and Structures, 25(4), 045013.